SCIENTIFIC REPORTS

OPEN

SUBJECT AREAS:
DNA
BIOMATERIALS

Received
21 July 2014

Accepted
14 November 2014

Published
19 December 2014

Correspondence and requests for materials should be addressed to F.X. (xiafan@hust.edu.cn)

A Fluorescence-Quenching Platform based on Biomineralized Hydroxyapatite from Natural Seashell and Applied to Cancer Cell Detection

Ying Zhang[1,2], Wei Liu[2], Craig E. Banks[3], Fei Liu[1], Mao Li[1], Fan Xia[1] & Xiangliang Yang[2]

[1]Key Laboratory for Large-Format Battery Materials and System, Ministry of Education, School of Chemistry & Chemical Engineering, [2]National Engineering Research Center for Nanomedicine, College of Life Science &Technology, Huazhong University of Science & Technology, 1037 Luoyu Road, Wuhan 430074, P.R.China, [3]Faculty of Science and Engineering, School of Chemistry and the Environment, Division of Chemistry and Environmental Science, Manchester Metropolitan University, Chester Street, Manchester M1 5GD, Lancs, UK.

As a typical biomineral, hydroxyapatite (HAp) is widely applied in bone implants and other related fields. However, the inherent nature of HAp can potentially be altered through restricting its fabrication conditions. Here, HAp fabricated by a hydrothermal treatment of pieces of natural seashell is demonstrated to have the capability of fluorescence quenching. To the best of the author's knowledge, this is the first time that this new property of HAp has been reported. Consequently, we assembled a fluorescence-quenching platform based on the biomineralized HAp substrate following a hydrothermal treatment and associated with a DNA molecular beacon and applied to cancer cell detection by the transformation from "OFF state" (fluorescence quenching) to "ON state" (fluorescence recovery). Herein, we found that the outer surface of HAp material after hydrothermal biomineralization for 5 days has considerable capability for both fluorescence quenching and recovery. These results may also have implications in the further detection of various targets such as cancer cells with other special surface antigens, significant biological small molecules or disease related microRNA, just by changing the sequence of the nucleic acid beacon according to the corresponding aptamer.

Biomineralization is a common bioprocess occurring in nature and plays an important role in the fabrication of biological hard tissues[1]. Inspired by nature, unique, effective strategies are exploited to fabricate functional materials with intricate structures[2]. In terms of taxonomic distribution, the most common biominerals are the phosphate and carbonate salts of calcium that are used in conjunction with organic polymers such as collagen and chitin to give structural support to bones and shells[3]. Wherein, the mollusc shell is a biogenic composite material typically consisting of 95~99% $CaCO_3$ by weight and 1~5% organic macromolecules, which has been the subject of much interest in materials science because of its unusual properties and its model character for biomineralization[4]. Owing to the sufficient amount of this biomass, the conversion of natural sea-shell pieces to HAp ($Ca_{10}(PO_4)_6(OH)_2$,) has been explored as a convenient strategy for the fabrication[5]. It is important to note that with the development of materials science and technology, more and more unique properties of HAp have been recognized and thus its application has been extended from a traditional biomedical material used in bone implants into wider applications such as vectors in gene therapy, environmental decontamination, biosensor, and many others[6–8], attributed to the unique crystalline structure with elaborated 3D networks. For example, we have synthesized biomimetic HAp with special microstructures by the assistance of natural biomass such as eggshell, eggshell membrane and bamboo membrane, which has been demonstrated to exhibit excellent electrochemical sensitivity toward toxic heavy metal ions and organics in polluted environments[9–11]. Additionally, the relationship between crystalline structure and phase composition and its electrochemical sensing capability has been clarified. Such work indicates the possibility that the 3D networks of HAp crystalline lattice can be controlled by restricting the conditions of biomineralization; hence the inherent nature/properties of biomimetic HAp can be tailored for a range of applications.

Consequently, in this communication, we report the fabrication of a HAp material via a hydrothermal treatment strategy originating from natural seashell pieces. The usefulness of this bespoke fabricated material is demonstrated to exhibit a fluorescence quenching capability. Furthermore by combining the excellent biocompatibility and the new feature of this material, we sought to construct a fluorescence detection platform combined with nucleic acid molecular beacon technique and have applied it for the detection of cancer cells by fluorescent quenching and recovery. To the best of our knowledge, this is the first report that the traditional biomaterial (HAp via a hydrothermal treatment from seashell pieces) is utilized as fluorescence detection platform and used for cancer cell detection. Our approach allows the development of a new and cost-efficient fluorescence detection platform.

Experimental

Fabrication of HAp by hydrothermal biomineralization strategy. All the reagents were purchased from Acros and used without any purification. All the solutions were prepared using ultra-pure water (>18.2 MΩ) from Millipore Synergy system (AMETEK, UK). The shell of Colossal False Fusus (a common sea-shell originating from the Philippines) was broken into ~1 cm × 1 cm pieces and ultrasonic cleaned by ultra-pure water and anhydrous ethanol for 30 minutes. After being air-dried at 40°C for 2 hours, the shell pieces were added into autoclaves respectively containing 80 mL of $NH_4H_2PO_4$ solution (0.12 g/mL). The autoclaves were then sealed and heated at 160°C in a thermostat for 3~9 days. After this step, the products were filtered and alternately washed with ultra-pure water/anhydrous ethanol. Following this, the samples were air-dried at 60°C for 12 hoursand characterized with Field Emission Scanning Electron Microscope (FESEM; NOVA NANOSEM 230) equipped with EDAX Genesis, X-Ray Diffraction meter (XRD), and Attenuated Total Reflectance-Fourier Transform Infrared Spectroscopy (ATR-FTIR; Bruker VERTEX-70) in order to identify the evolution of morphology, element composition crystalline phrase and surface functional groups for both the outer and inner surfaces after the duration from 3 to 9 days.

Surface grafting with DNA molecule beacons. The DNA molecule beacon used in this experiment was synthesized and modified by TaKaRa Biotech (Dalian, China), with the sequence listed as below (5′-3′): FAM-AGCGCCACTACAGAGGTTG-CGTCTGTCCCACGTTGTCATGGGGGGTT GGCCTGGCGCTT-NH_2 (The underlined sequence is the corresponding aptamer to the EpCAM.) All the solutions and vessels were used after heat sterilization treatment. Firstly, the DNA molecule beacons were prepared into 100 μM stocking solution in 1×TE Buffer (pH 7.5~8.0) and diluted to 1 μM for used by adding a certain volume of TE Buffer. Then an as-prepared HAp substrate was immersed into 1 mL of beacon solution, and grafted in a Thermomixer comfort (Eppendorf) at 37°C for 12 hours. Consequently, the DNA-modified HAp substrate was taken out and washed with 1 × PBS to remove the dissociative DNA.

Construction of fluorescence detecting platform and application for cancer cell detection. The EJ bladder cancer cell line (EpCAM positive, donated by Tongji Medical College) was chosen in this research. For cell culture, RPMI-1640 growth medium and trypsin were obtained from Invitrogen (Gibco® Life Technologies). Multi-Cell® Fetal Bovine Serum (FBS) was obtained from Wisent. The anchorage-dependent cells were digested to suspensions by adding certain volumes of 0.25% trypsin. Cell counts were determined by counting three aliquots of cells using a hemacytometer. The functionalized substrates were placed into a size-matched 4-well Lab-TekTM Chamber Slide (Thermo Fisher Scientific), and then 1 mL cell suspensions (10^5 cells/mL) were respectively loaded. After incubating for 45 min at 37°C and 5% CO_2, the platform was gently washed with PBS at least three times. The substrates were then taken out and loaded onto a cleaned glass slide. The results were characterized by an inversed fluorescence microscope (Olympus, IX71) by chromatic discrimination of the substrate surfaces before and after cell capture (excitation wavelength: ~365 nm). In order to better determine the position of captured cells, we added an extra step for cell staining by DAPI (Invitrogen). The hybridization of DNA chain and target cancer cells was illustrated by a confocal microscopy (Zeiss, LSM 700) (excitation wavelength: 340 nm for DAPI and 490 nm for 5′-FAM).

Results and discussion

During the hydrothermal treatment process, both the outer and inner surfaces of the original seashell experience a series of morphology evolutions, as illustrated in Fig. 1, which suggests both the two surfaces are composed with little fractals, and those on the inner surface are relatively homogeneous, corresponding with its smoother appearance than the outer surface. After 3 days' biomineralization, flower-like crystalline clusters have formed on the outer surface consistinh of microsheets with a length of ~30 μm and a width of

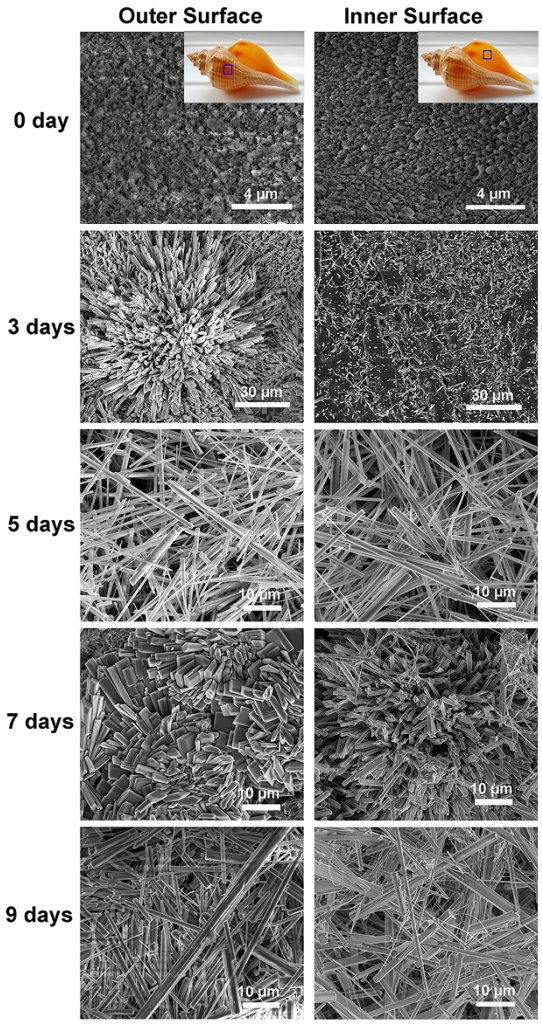

Figure 1 | Morphology evolution of the natural seashell after hydrothermal biomineralization at 160°C for 3~9 days. The outer and inner surfaces were examined separately using SEM. The inserted chromatic photographs are initial appearance of *Colossal False Fusus*, with rectangular boxes marked the outer and inner surfaces, respectively.

~3 μm, while the small crystals on the inner surface are sparse and straggly. However, after 5 days, the crystal grown on the two surfaces are microwires, with a length of ~50 μm and a width of ~2 μm. Furthermore, increasing the biomineralization time to 7 and 9 days, a transformation occurs into another flower-like cluster and then backs into a microwire formation. Different from the first one, the 7 day-flower-like clusters grown on the outer surface are constructed by microblocks while those on the inner are fabricated by micropillars. Additionally, both the 9 day-microwires have longer lengths than the 5 day-samples. In nature, one secret of biominerals' superior material properties is their organic–inorganic hybrid structure whereby precise arrangement of the building blocks is achieved over several length scales[12]. This principle has been reflected by fractal dimension calculations for both surfaces and suggests distinct evolvement processes in the duration time (see Fig. S1 of the Supporting Information (SI)). In view of the same piece of seashell, this evolutional difference is supposed to be due to their distinct organic composition[13–15]. EDAX characterization was utilized to investigate the evolution of element composition (see Fig. S2 of SI). The corresponding Ca:P ratio is also summarized here, with the outer surface of 3 day-HAp exhibiting the highest Ca:P ratio value of 2.62.

Additionally, X-ray diffraction characterization was carried out for crystalline phase identification (see Fig. S3 of SI) and reveals that

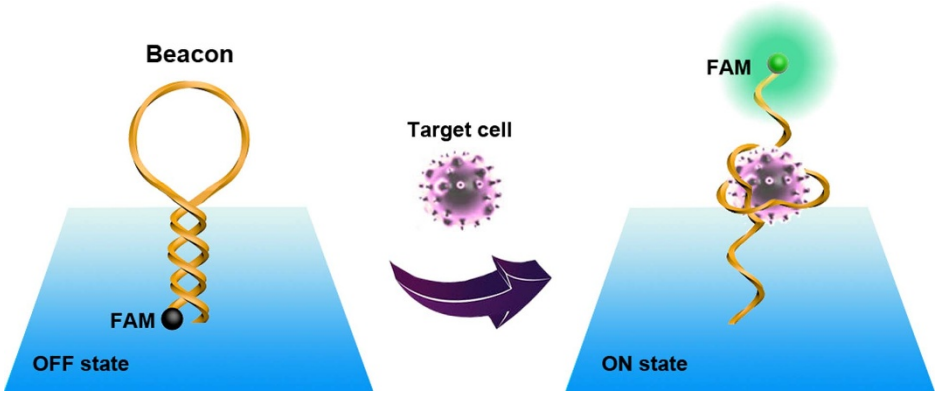

Figure 2 | Schematic illustration of the proposed biomimetic platform. In the absence of target cells, the beacon maintains a loop-stem structure, and fluorescence is quenched as a result of the close proximity between fluorophores and HAp quencher (OFF state). Otherwise, the conformation of the DNA probe will alter and interact with EpCAM in cell membrane, causing the fluorophores to move far enough away from the HAp quencher to result in restoration of fluorescence signal (ON state).

both the surfaces of 3 days-sample mainly consisted of monetite ($CaHPO_4$), but the outer surface contains a certain of HAp ($Ca_5(PO_4)_3OH$). However, when the hydrothermal treatment time was extended to 5∼9 days, all the surfaces are constructed by HAp and calcium hydrogen phosphate hydroxide ($Ca_9H(PO_4)_6OH$). The discrepancy of quenching capability amongst the crystals obtained after 5∼9 days' hydrothermal treatment could be attributed to the difference of HAp proportions in the crystalline phases. Furthermore, it is accepted that for a variety of calcium phosphate compounds, the Ca:P ratio might be used to roughly estimate the phase composition of the surface. Typically, the ratios for the three compounds mentioned above are 1 (for $CaHPO_4$), 1.67 (for $Ca_5(PO_4)_3OH$) and 1.5 (for $Ca_9H(PO_4)OH$), respectively. Considering the corresponding Ca:P ratio of different crystalline samples, only the 5 days-crystal on the outer surface (Ca:P = 1.68) is close to ratio of 1.67. As a result of this, it can be considered that only the outer surface of 5 days-crystal was mainly composed by HAp phase.

Subsequently, the biomimetic HAp fluorescence-quenching platform was constructed by grafting 5′FAM-modified DNA probe (beacon) on the surface and applied for cancer cell determination (Fig. 2). Herein, the beacon was designed to be capable of specifically hybridizing with EpCAM, which has been known as a trans-membrane glycoprotein that is frequently overexpressed in a variety of solid-tumour cells (EpCAM positive cells)[16,17]. As shown in Fig. 3, it can be obviously observed in the fluorescence photographic images that the outer surface of 3 days-HAp has the capability for quenching most of 5′-FAM fluorophores. When it is hybridized with target cells, not all the fluorescence signal was able to be recovered and the reaction between DNA beacon and EpCAM on the cell membrane was confirmed by confocal microscopy characterization. In contrast, the 5 days-HAp has considerable capability for both fluorescence quenching and recovery. We can see obvious "OFF state" to "ON state" variation process. However, the quenching capability decreased gradually when the hydrothermal duration time further delayed. For instance, we can hardly find the mentioned transformation on the 9 days-HAp platform. On the other hand, we also have difficult to find this on the inner surface for all the samples, as shown in Fig. S4 of SI. Although confocal microscopy characterization still provides evidence for the beacon-cell reaction occurred on the surface of HAp, this determination results should be classified as ineffective.

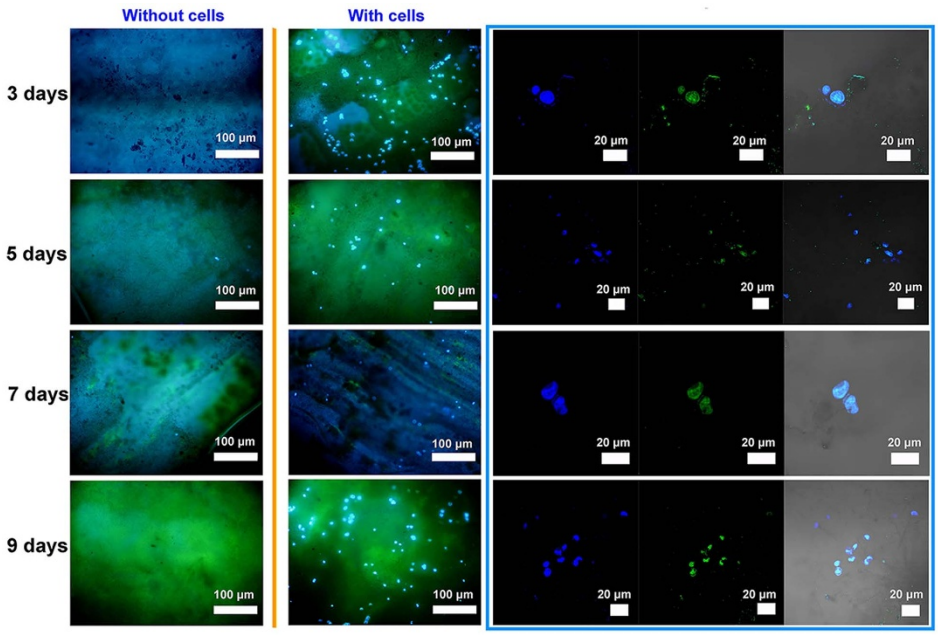

Figure 3 | Inverted Fluorescence Microscope (IFM) and Laser Scanning Confocal Microscopy (LSCM) images of biomimetic substrates before and after cell capture for the outer surface after hydrothermal treated for 3∼9 days.

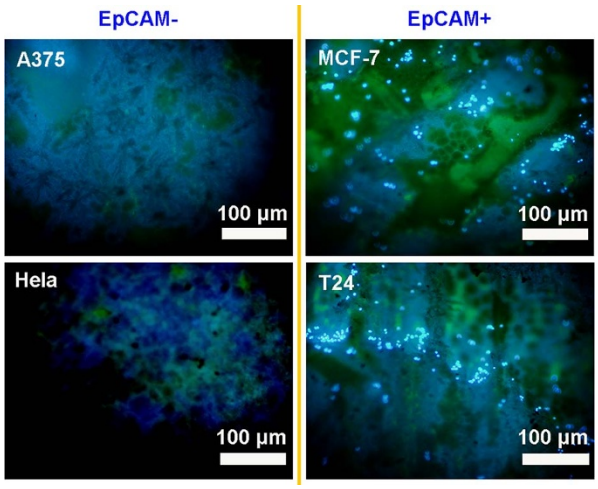

Figure 4 | **IFM images of biomimetic substrates after respectively capture of other EpCAM+ (MCF-7 and T24) and EpCAM– (A375 and Hela) cells (stained by DAPI) for the outer surface after hydrothermal treated for 5 days.**

Based on these results, the specificity was confirmed by the invalid determination of EpCAM– cells (e.g. A375 and Hela) compared with effective detection of other EpCAM+ cells (e.g. MCF-7 and T24) by the outer surface of 5 day-HAp (Fig. 4).

This approach is a universal strategy for achieving the detection of different targets such as cancer cell with other special surface antigens, significant biological small molecule or disease related microRNA; one just needs to change the sequence of the nucleic acid beacon according to the corresponding aptamer or complementary strand. However, a limitation of this strategy is that associated with the natural heterogeneity of biomaterials, which may lead to the asymmetrical quenching capability of local regions even on the same surface. In order for practical applications, further optimization of experimental conditions is of the essence.

In terms of the fluorescence quenching mechanism, as far as we know, molecular collisions between the fluorophores and quencher occurring during the excited state lifetime of the fluorophores give rise to dynamic quenching, while formation of a non-fluorescent complex between the two species gives rise to static quenching[18]. According to classical nucleation theory[19], the crystallization of inorganic minerals starts from their constituting ions, which, on the basis of their ionic complementarity, form small clusters in a stochastic process of dynamic growth and disintegration. These clusters become stable when a critical size is reached at which the increasing surface energy related to the growing surface area is balanced by the reduction of bulk energy related to the formation of a crystal lattice. The resulting primary nanoparticles form the critical crystal nuclei that are the basis of further growth through the associated reduction of the *Gibbs* free energy of the system. It is possible that the crystal lattice of inorganic minerals can be adjusted by controlling the environment of crystal nucleation and growth. Therefore, it is reasonable that the hydrothermal biomineralization strategy under certain con-

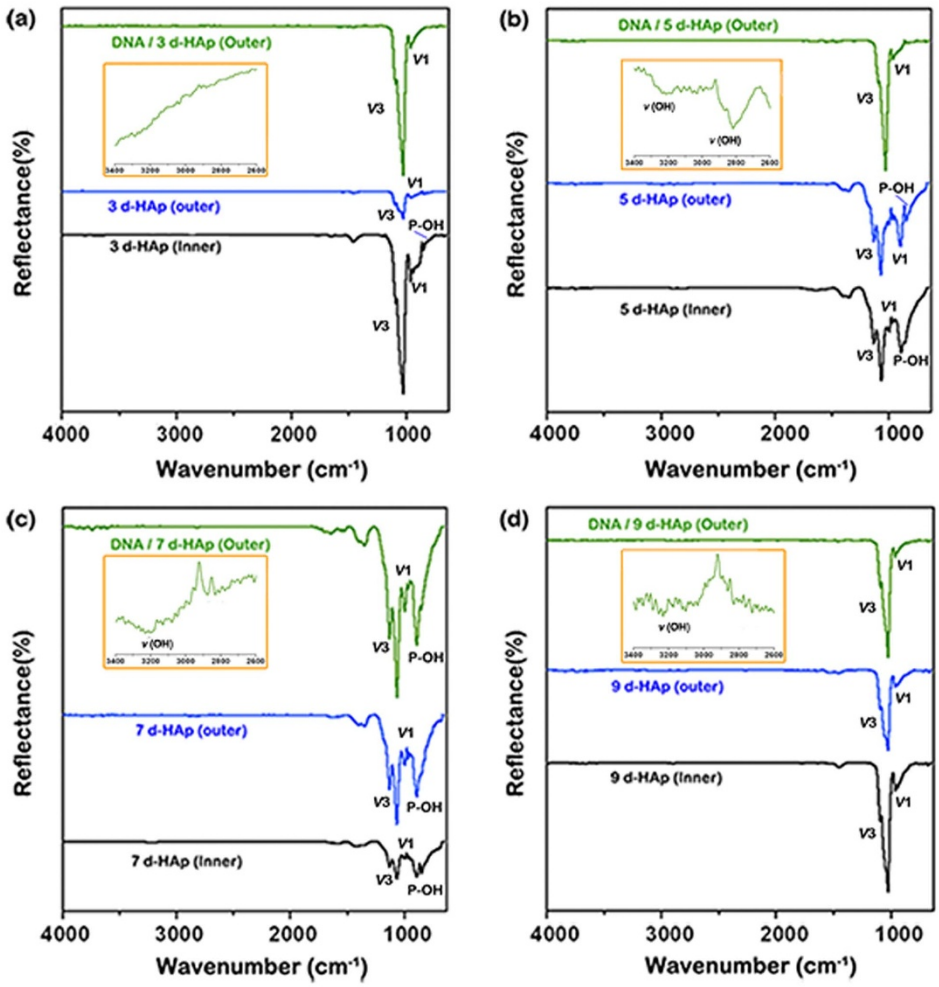

Figure 5 | **ATR-FTIR characterization for the functional groups on the surface of (a–d) 3 d~9 d HAp samples before and after DNA bonding.**

ditions (such as duration time and composition of biosubstrates) is able to fabricate appropriate crystalline structures of HAp so that 5′-FAM can bond to the surface and form a non-fluorescent 5′-FAM-HAp complex by electrostatic interaction. This speculation was supported by the results from ATR characterization, shown in Fig. 5. Herein, it is obvious to notice that the spectroscopy curves for all the samples before DNA bonding, a number of characteristic bands representing the phosphate group at 1100∼1000 cm^{-1}(ν_3 triply asymmetric stretching mode of the P-O bond) and ∼963 cm^{-1} (ν_1 symmetric stretching mode of the P-O bond) for both outer and inner surface. Bands at ∼3300 cm^{-1} and 1631 cm^{-1} in IR spectrum are due to O–H stretching and ν_2 (H–O–H) bending modes of lattice water molecule. The band at 896∼900 cm^{-1} could be attributed to the P-OH deformation indicating the protonation of the phosphate groups[20]. Additionally, bands in the 1630∼1191 cm^{-1} region indicate the existence of carbonate groups, suggesting their incorporation into the crystal structure of HAp, which was possibly due to the absorption of carbon dioxide from the air during the holding time. According to the XRD identification (Fig. S3), the difference amongst these spectroscopy curves could be attributed to the evolution of crystalline composition during a holding time from 3 days to 9 days. However, only the spectroscopy shape of 5 d-sample verified remarkably after DNA bonding to the surface, and the curves for the other samples almost stay the same. It was suggested that non-fluorescent FAM-HAp complex only formed on the outer surface of 5 d-sample when bonding with FAM-DNA beacon and the holding time of 5 days is suitable to fabricate the platform with fluorescence quenching capability.

Although these characterizations primarily confirm the proposed mechanism, after all, further researches are still requested to identify the exact quenching mechanism in the future, with ultra-detailed material characterizations by advanced technologies.

Conclusions

In summary, we have assembled a fluorescence quenching platform based on a HAp substrate fabricated by a simple hydrothermal treatment of natural sea-shell pieces in a solution of ammonium phosphate and further applied it for cancer cell detection. The switchable fluorescence quenching capability depends on the distance of fluorophore and the surface of HAp. Herein, we found the outer surface of 5 days-HAp has considerable capability for both fluorescence quenching and recovery. Future work will include application of this fluorescence-quenching platform for the detection of other targets. Additionally, more intensive researches are still required for exactly identifying the quenching mechanism of this material.

1. Kunz, W. & Kellermeier, M. Beyond biomineralization. *Science* **323**, 344–345 (2009).
2. Kim, S. J. & Park, B. C. Bio-inspired synthesis of minerals for energy, environment, and medicinal applications. *Adv. Funct. Mater.* **23**, 10–25 (2013).
3. Vinn, O. Occurrence, formation and function of organic sheets in the mineral tube structures of serpulidae (polychaeta, annelida). *PLoS One* **8**, e75330 (2013).
4. Li, X. & Zeng, H. Calcium carbonate nanotablets: bridging artificial to natural nacre. *Adv. Mater.* **24**, 6277–6282 (2012).
5. Vecchio, K. S., Zhang, X., Massie, J. B., Wang, M. & Kim, C. W. Conversion of bulk seashells to biocompatible hydroxyapatite for bone implants. *Acta Biomaterialia* **3**, 910–918 (2007).
6. Srinivasan, M., Ferraris, C. & White, T. Cadmium and lead ion capture with three dimensionally ordered macroporous hydroxyapatite. *Environ. Sci. Technol.* **40**, 7054–7059 (2006).
7. Salimi, M. N. & Anuar, A. Characterizations of biocompatible and bioactive hydroxyapatite particles. *Procedia Eng.* **53**, 192–196 (2013).
8. Wang, B., Zhang, J., Pan, Z., Tao, X. & Wang, H. A novel hydrogen peroxide sensor based on the direct electron transfer of horseradish peroxidase immobilized on silica-hydroxyapatite hybrid film. *Biosens. Bioelectron.* **24**, 1141 (2009).
9. Zhang, Y., Liu, Y., Ji, X., Banks, C. & Zhang, W. Flower-like hydroxyapatite modified carbon paste electrodes applicable for highly sensitive detection of heavy metal ions. *J. Mater. Chem.* **21**, 7552–7554 (2011).
10. Zhang, Y., Liu, Y., Ji, X., Banks, C. & Zhang, W. Conversion of egg-shell to hydroxyapatite for highly-sensitive detection of endocrine disruptor bisphenol A. *J. Mater. Chem.* **21**, 14428–14431 (2011).
11. Zhang, Y., Liu, Y., Ji, X., Banks, C. & Zhang, W. Sea cucumber-like hydroxyapatite: cation-exchange membrane assisted synthesis and application for ultra-sensitive heavy metal detection. *Chem. Commun.* **47**, 4126–4128 (2011).
12. Cölfen, H. Biomineralization: a crystal-clear view. *Nat. Mater.* **9**, 960–961 (2010).
13. Li, X. & Zeng, H. Calcium Carbonate Nanotablets: Bridging Artificial to Natural Nacre. *Adv. Mater.* **24**, 6277–6282 (2012).
14. Kim, S. & Park, C. Mussel-inspired transformation of $CaCO_3$ to bone minerals. *Biomaterials* **31**, 6628–6634 (2010).
15. Asenath-Smith, E., Li, H., Keene, E., Seh, Z. & Estroff, L. Crystal growth of calcium carbonate in hydrogels as a model of biomineralization. *Adv. Funct. Mater.* **22**, 2891–2914 (2012).
16. Wang, S. *et al.* Three-dimensional nanostructured substrates toward efficient capture of circulating tumour cells. *Angew. Chem. Int. Ed.* **48**, 8970–8973 (2009).
17. Rao, C. *et al.* Expression of epithelial cell adhesion molecule in carcinoma cells present in blood and primary and metastatic tumors. *Int. J. Oncol.* **27**, 49–57 (2005).
18. Chen, H., Ahsan, S., Santiago-Berrios, M., Abruña, H. & Webb, W. Mechanisms of quenching of alexa fluorophores by natural amino acids. *J. Am. Chem. Soc.* **132**, 7244–7245 (2010).
19. Ehrlich, H. *Biological Materials of Marine Origin: Invertebrates* [Gorb. S. (ed.)](Springer, Heidelberg, 2010).
20. Socrates, G. *Infrared and Raman Characteristics Group Frequencies* (John Wiley & Sons Ltd, Chichester, 2001).

Acknowledgments

This work was supported by Special Financial Grant and 2-class General Financial Grant from the China Postdoctoral Science Foundation (2013T60720 and 2012M521431), Initiatory Financial Support from HUST, National Basic Research Program of China (973 program, 2012CB932500, 2013CB933000 and 2015CB932600), 1000 Young Talent (to Fan Xia), and the National Natural Science Foundation of China (21375042 and 21405054). The authors thank the HUST Analytical and Testing Center and National Laboratory for Optoelectronics for allowing us to use their facilities and Xihang Liu for drawing the schematic models.

Author contributions

Y.Z. and F.X. designed the experiment, analyzed the data. F.L. and M.L. performed the experiment. Y.Z. wrote the paper. W.L., C.E.B. and X.L.Y. offered valuable comments. C.E.B. did much work for paper polishing.

Additional information

Supplementary information accompanies this paper at http://www.nature.com/scientificreports

Competing financial interests: The authors declare no competing financial interests.

How to cite this article: Zhang, Y. *et al.* A Fluorescence-Quenching Platform based on Biomineralized Hydroxyapatite from Natural Seashell and Applied to Cancer Cell Detection. *Sci. Rep.* **4**, 7556; DOI:10.1038/srep07556 (2014).